

Searching Beyond Gd for Magnetocaloric Frameworks: Properties and Interactions of the $Ln(HCO_2)_3$ Series

Paul J. Saines^{1*}, Joseph A. M. Paddison^{1,2}, Peter M. M.
Thygesen¹ and Matthew G. Tucker²

Department of Chemistry, University of Oxford
Inorganic Chemistry Laboratory, South Parks Road
Oxford OX1 3QR, U.K.

ISIS Facility, Rutherford Appleton Laboratory
Harwell Oxford, Dicot, OX11 0QX, U. K.

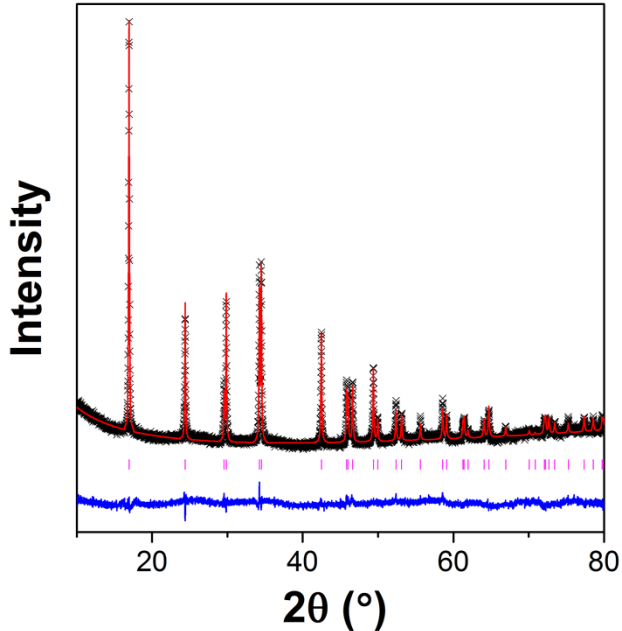


Fig. S1: Conventional powder X-ray diffraction pattern of $\text{Gd}(\text{HCO}_3)_3$ fitted using the Rietveld method, highlighting the purity of the sample. The crosses, upper and lower lines are experimental and calculated intensities and the difference plot. The vertical markers indicate the positions of the Bragg reflections. R_p , R_{wp} and χ^2 of 2.90 %, 3.62 % and 2.13 are obtained, respectively from the refinement with $a = 10.4802(2)$ Å, $c = 3.98911(9)$ Å and a unit cell volume of $379.44(14)$ Å³. The high background in this diffraction pattern is from the fluorescence due to the Gd L-edges.

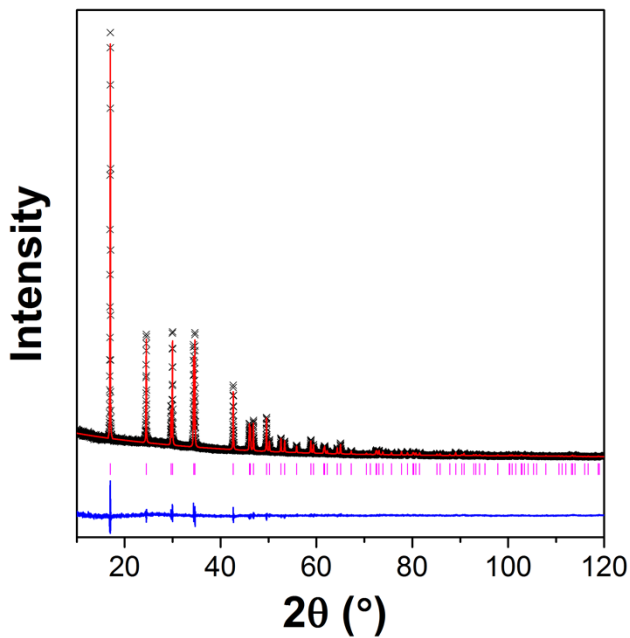


Fig. S2: Conventional powder X-ray diffraction pattern of $\text{Tb}(\text{HCO}_3)_3$ fitted using the Rietveld method, highlighting the purity of the sample. The format is the same as Fig. S1. R_p , R_{wp} and χ^2 of 3.81 %, 4.87 % and 0.98 are obtained, respectively from the refinement with $a = 10.43591(14)$ Å, $c = 3.96939(5)$ Å and a unit cell volume of $374.382(14)$ Å³.

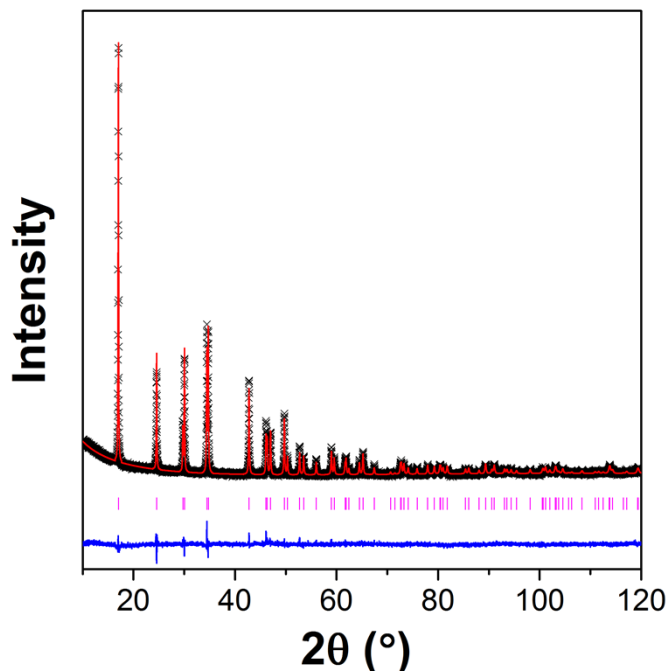


Fig. S3: Conventional powder X-ray diffraction pattern of $\text{Dy}(\text{HCO}_2)_3$ fitted using the Rietveld method, highlighting the purity of the sample. The format is the same as Fig. S1. R_p , R_{wp} and χ^2 of 2.38 %, 3.11 % and 1.80 are obtained, respectively from the refinement with $a = 10.412641(14)$ Å, $c = 3.95757(6)$ Å and a unit cell volume of 371.604(9) Å³.

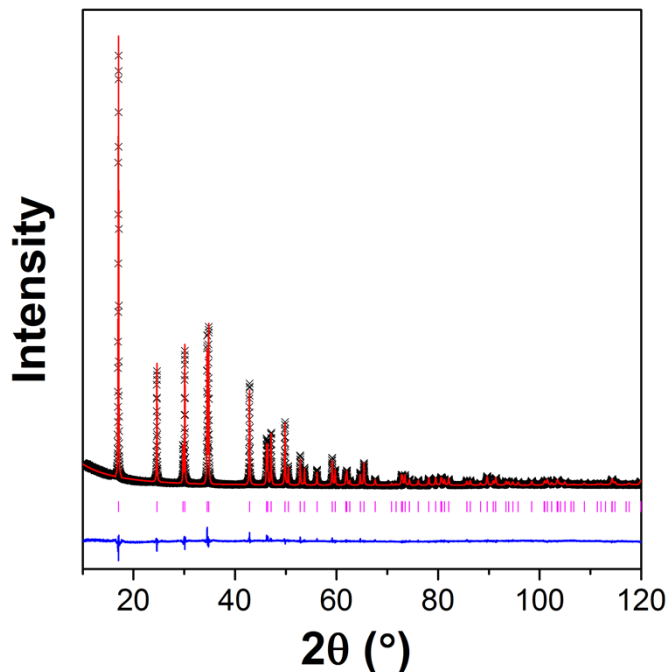


Fig. S4: Conventional powder X-ray diffraction pattern of $\text{Ho}(\text{HCO}_2)_3$ fitted using the Rietveld method, highlighting the purity of the sample. The format is the same as Fig. S1. R_p , R_{wp} and χ^2 of 6.66 %, 8.65 % and 3.97 are obtained, respectively from the refinement with $a = 10.38539(9)$ Å, $c = 3.94526(4)$ Å and a unit cell volume of 368.513(6) Å³.

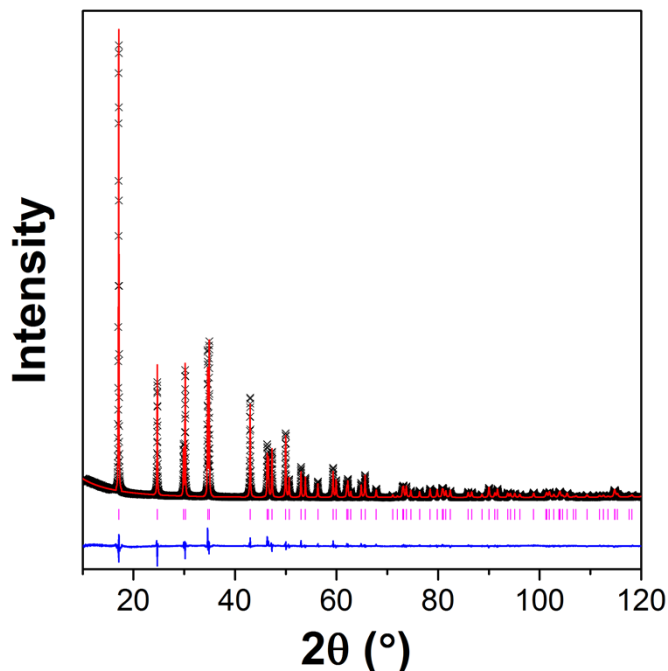


Fig. S5: Conventional powder X-ray diffraction pattern of $\text{Er}(\text{HCO}_2)_3$ fitted using the Rietveld method, highlighting the purity of the sample. The format is the same as Fig. S1. R_p , R_{wp} and χ^2 of 6.99 %, 9.10 % and 4.91 are obtained, respectively from the refinement with $a = 10.35786(7)$ Å, $c = 3.93231(3)$ Å and a unit cell volume of $368.357(5)$ Å³.

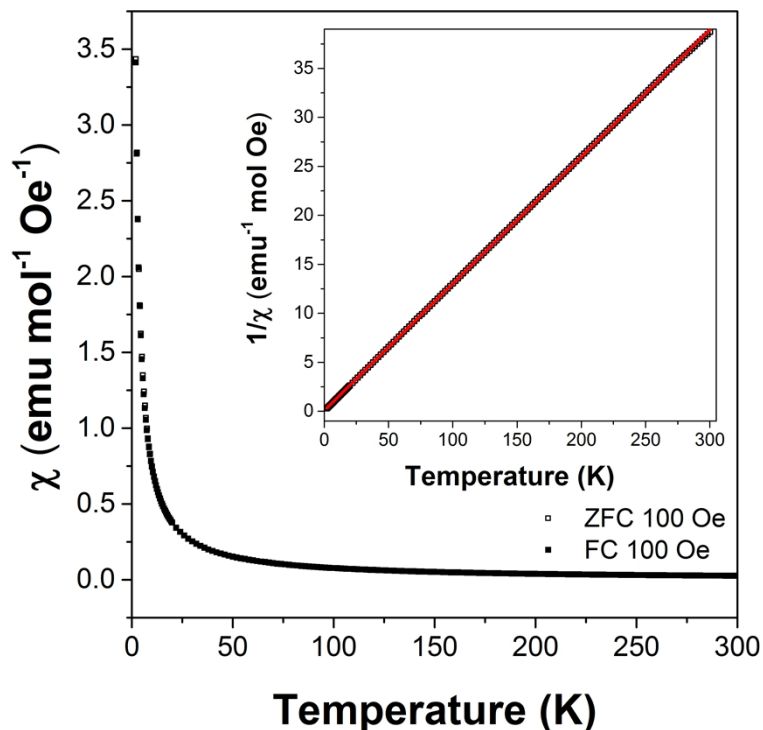


Fig S6: The main plot displays variable temperature Field cooled (FC) and Zero-Field cooled (ZFC) magnetic susceptibility measurements on $\text{Gd}(\text{HCO}_2)_3$ in a 100 Oe field. The insert shows a plot of $1/\chi$ versus temperature and a Curie-Weiss fit to it.

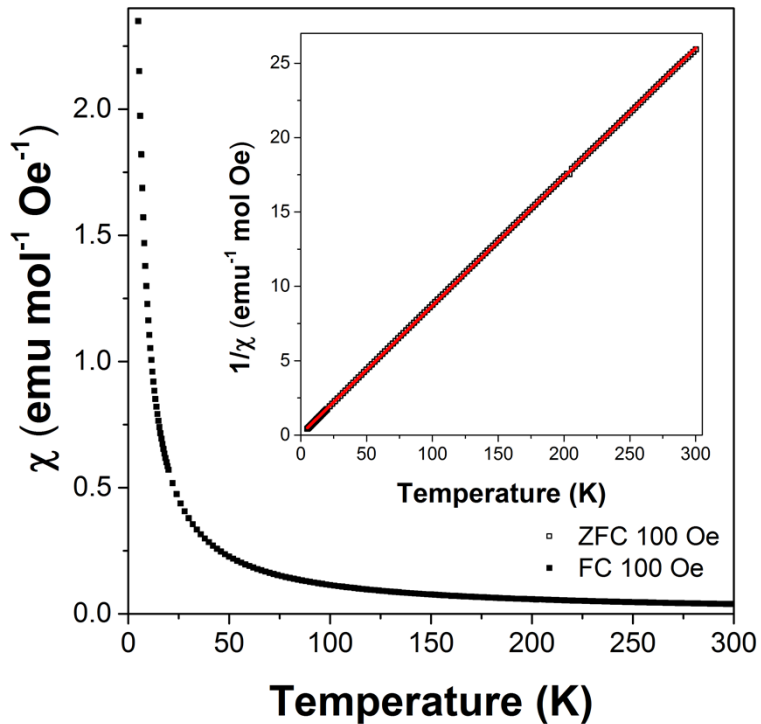


Fig S7: The main plot displays variable temperature FC and ZFC magnetic susceptibility measurements on $\text{Tb}(\text{HCO}_2)_3$ in a 100 Oe field. The insert shows a plot of $1/\chi$ versus temperature and a Curie-Weiss fit to it.

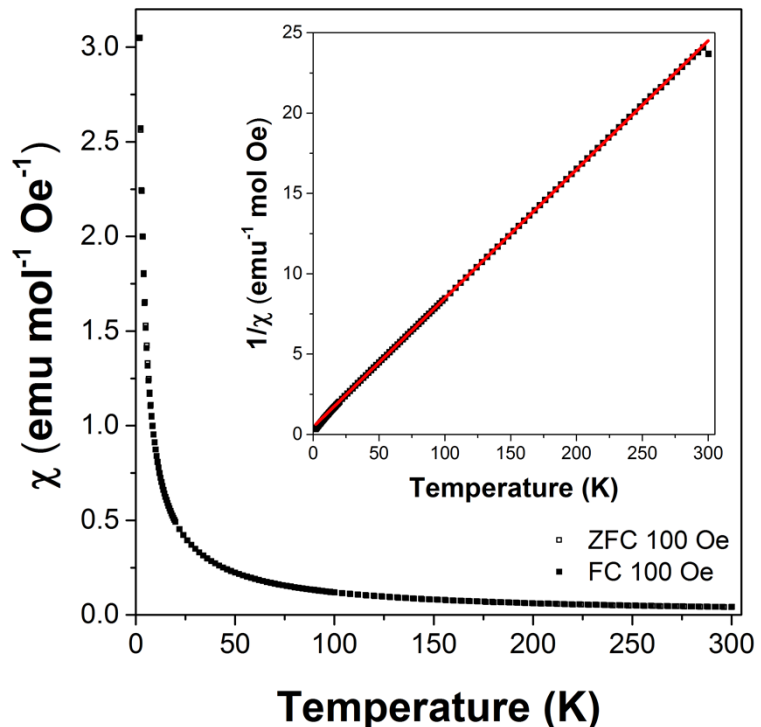


Fig S8: The main plot displays variable temperature FC and ZFC magnetic susceptibility measurements on $\text{Dy}(\text{HCO}_2)_3$ in a 100 Oe field. The insert shows a plot of $1/\chi$ versus temperature and a Curie-Weiss fit to the data obtained above 20 K.

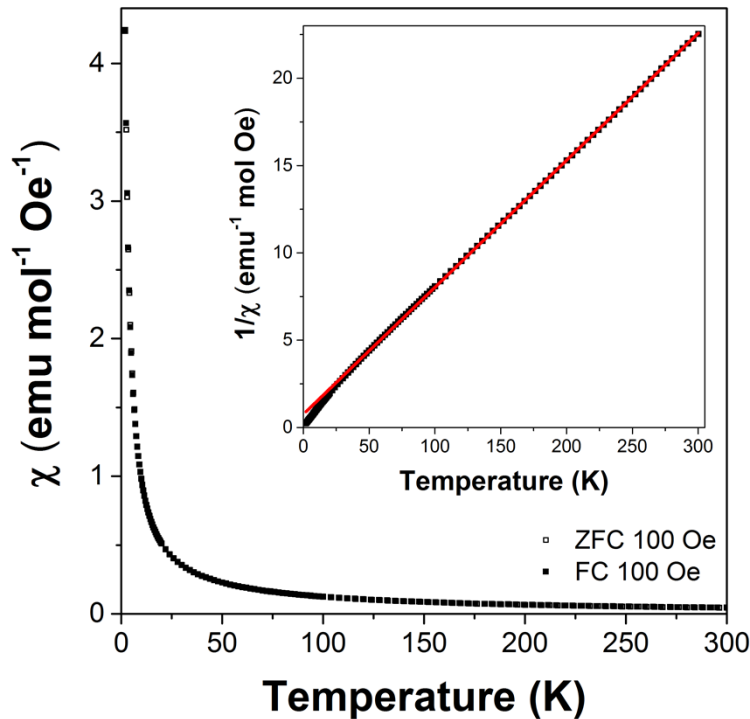


Fig S9: The main plot displays variable temperature FC and ZFC magnetic susceptibility measurements on $\text{Ho}(\text{HCO}_2)_3$ in a 100 Oe field. The insert shows a plot of $1/\chi$ versus temperature and a Curie-Weiss fit to the data obtained above 20 K.

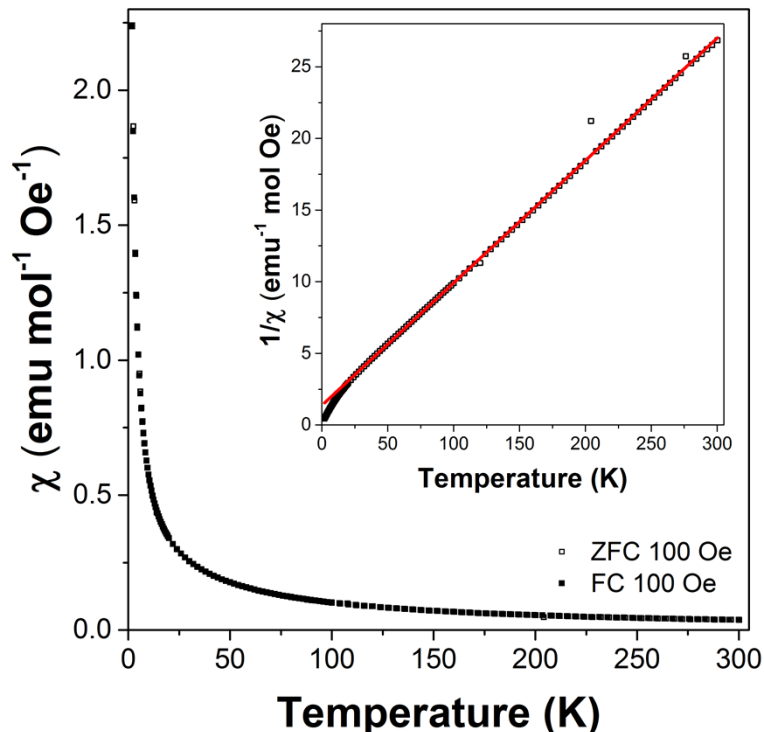


Fig S10: The main plot displays variable temperature FC and ZFC magnetic susceptibility measurements on $\text{Er}(\text{HCO}_2)_3$ in a 100 Oe field. The insert shows a plot of $1/\chi$ versus temperature and a Curie-Weiss fit to the data obtained above 24 K.

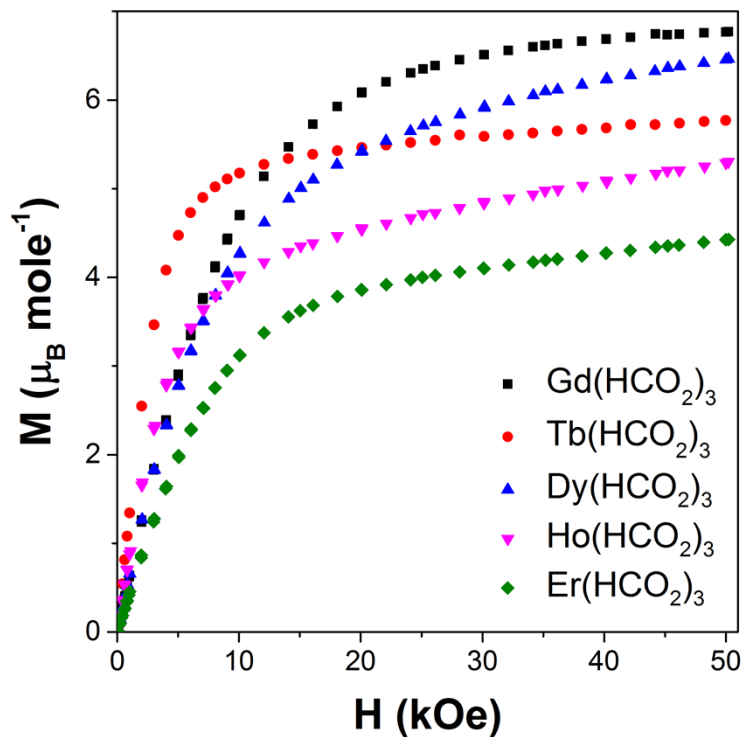


Fig. S11: Isothermal magnetisation measurements on the $\text{Ln}(\text{HCO}_2)_3$ frameworks measured at 2 K.

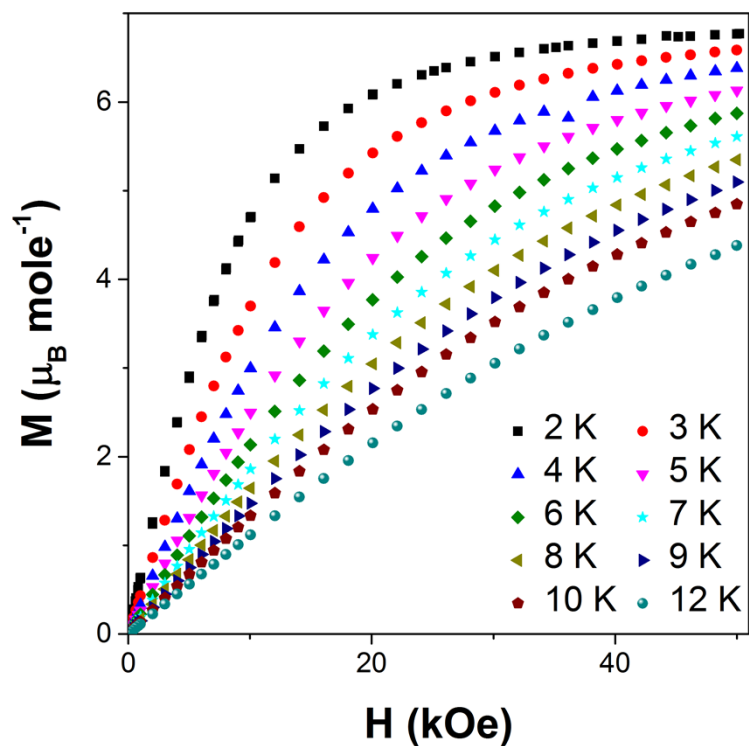


Fig. S12: Isothermal magnetisation measurements of the $\text{Gd}(\text{HCO}_2)_3$ framework.

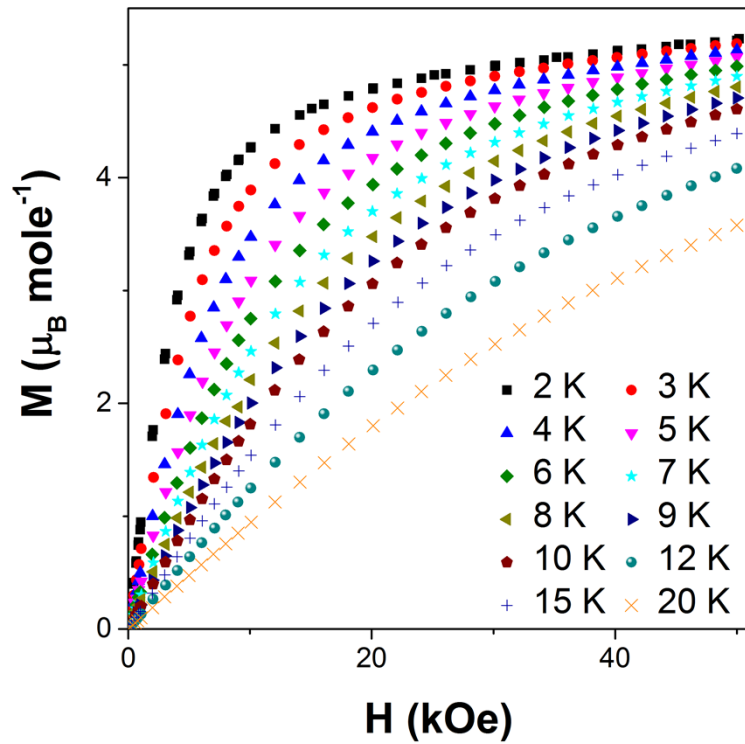


Fig. S13: Isothermal magnetisation measurements of the $\text{Tb}(\text{HCO}_2)_3$ framework.

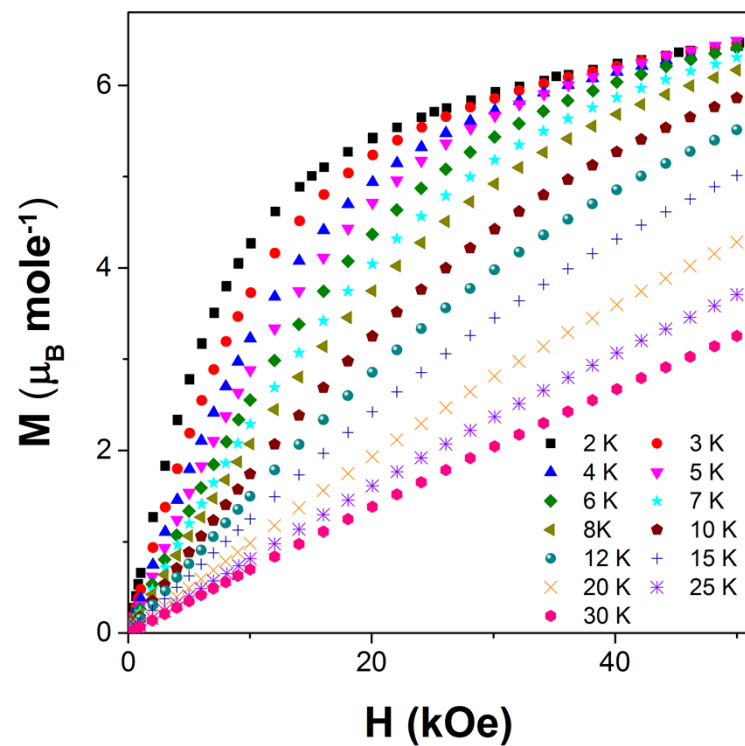


Fig. S14: Isothermal magnetisation measurements of the $\text{Dy}(\text{HCO}_2)_3$ framework.

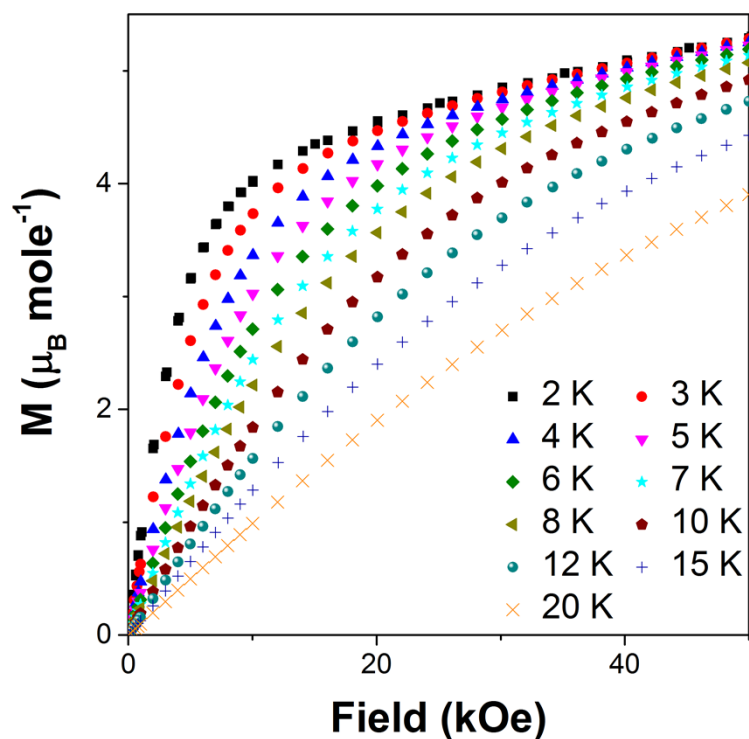


Fig. S15: Isothermal magnetisation measurements of the $\text{Ho}(\text{HCO}_2)_3$ framework.

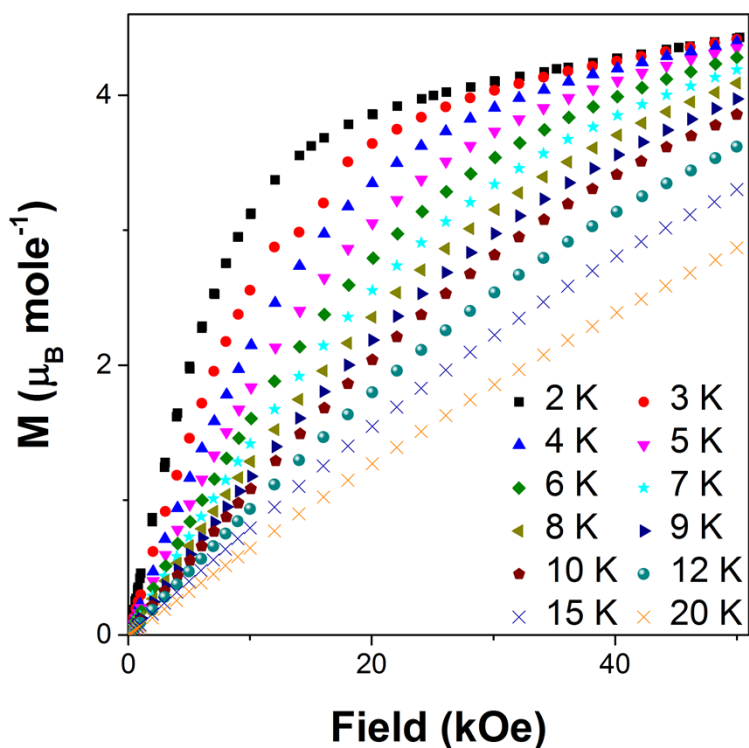


Fig. S16: Isothermal magnetisation measurements of the $\text{Er}(\text{HCO}_2)_3$ framework.

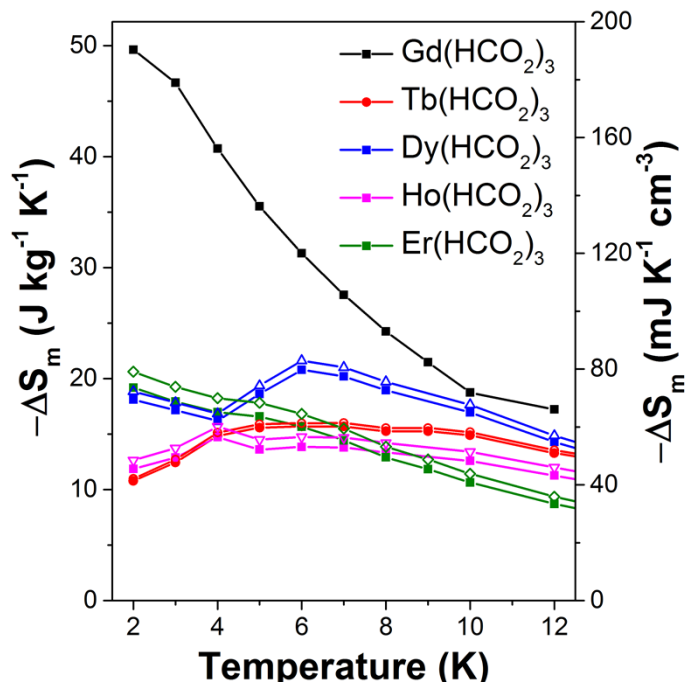


Fig. S17: Magnetic entropy change for a $\Delta B = 5\text{--}0 \text{ T}$ of the $Ln(\text{HCO}_2)_3$ frameworks. The filled symbols mark this per unit mass and the hollow in volumetric units.

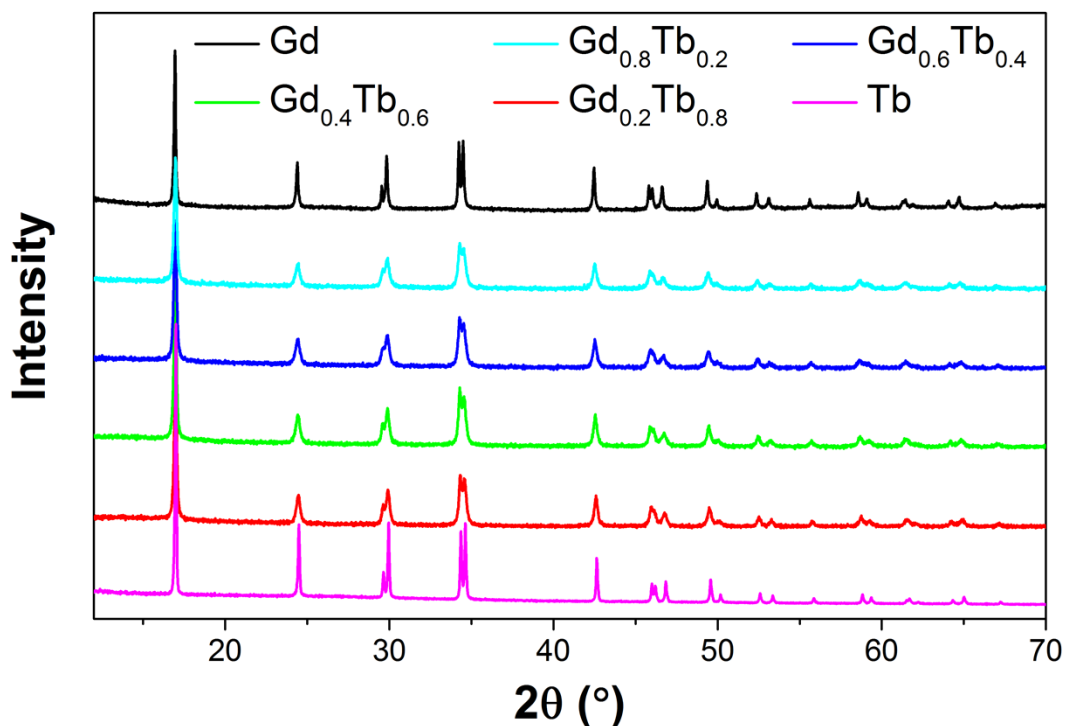


Fig S18: Diffraction patterns of the $Gd_{1-x}Tb_x(\text{HCO}_2)_3$ frameworks highlighting the purity of the doped samples and their broader peak shapes. The patterns are offset from each other for clarity.

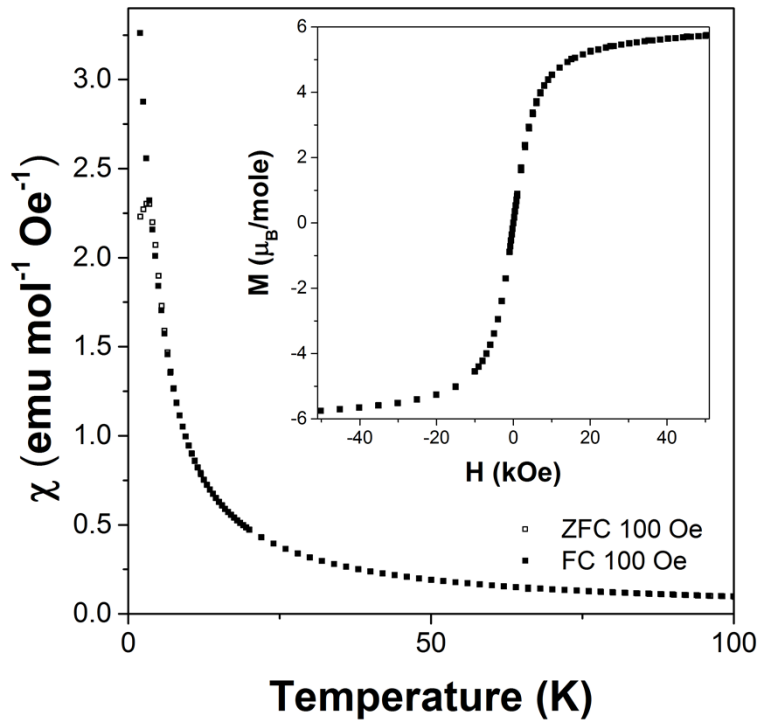


Fig S19: The main plot displays variable temperature FC and ZFC magnetic susceptibility measurements on $\text{Gd}_{0.4}\text{Tb}_{0.6}(\text{HCO}_2)_3$ in a 100 Oe field. The insert presents magnetization measurements carried out at 2 K.

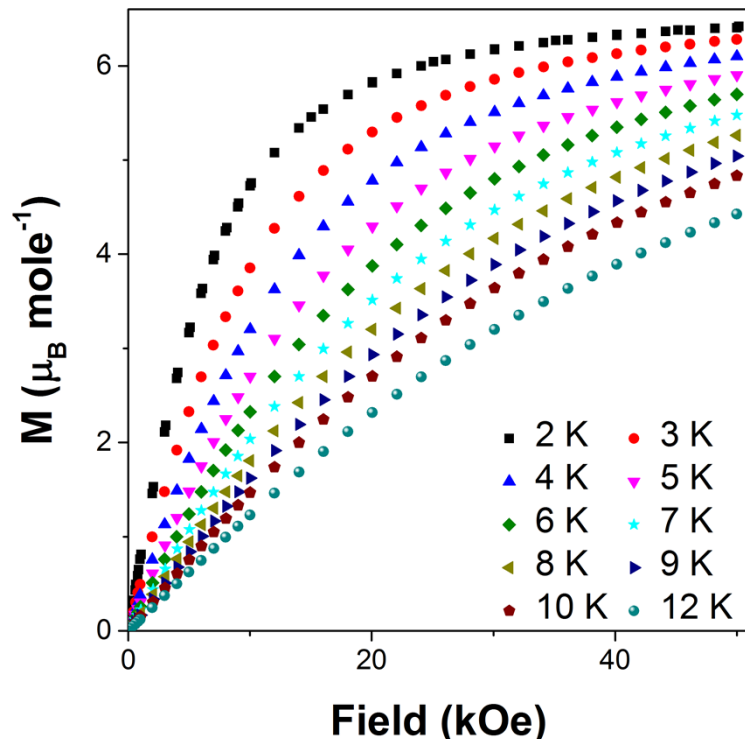


Fig. S20: Isothermal magnetisation measurements of the $\text{Gd}_{0.8}\text{Tb}_{0.2}(\text{HCO}_2)_3$ framework.

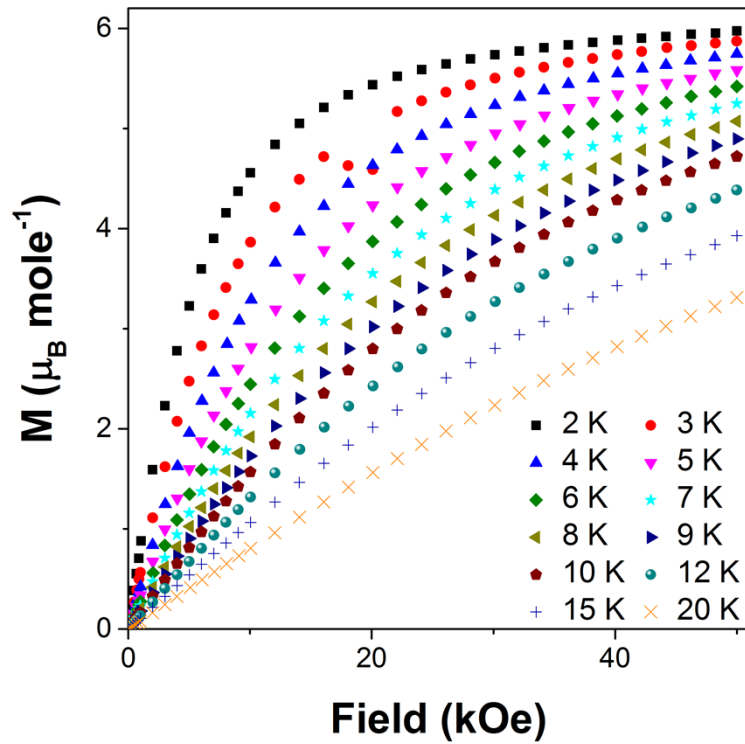


Fig. S21: Isothermal magnetisation measurements of the $\text{Gd}_{0.6}\text{Tb}_{0.4}(\text{HCO}_2)_3$ framework.

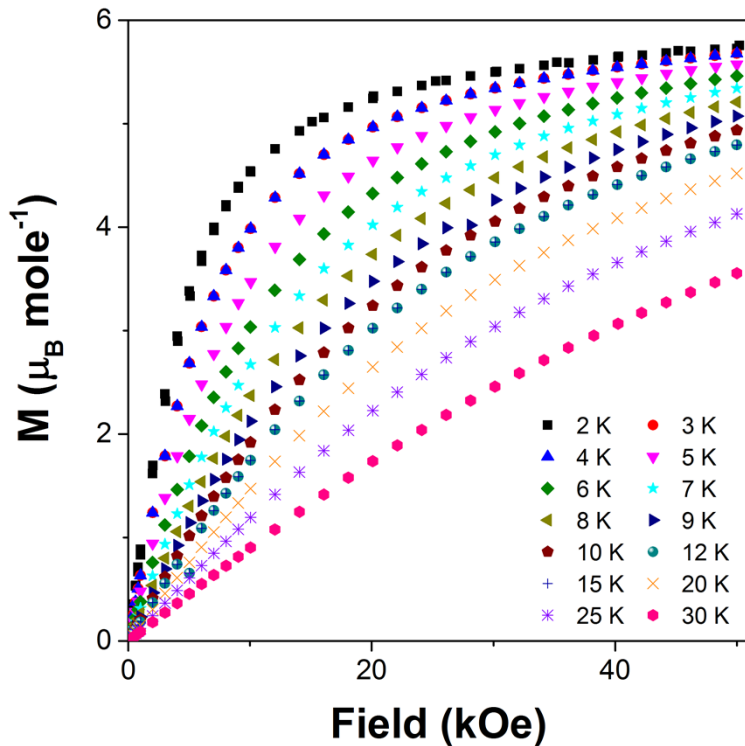


Fig. S22: Isothermal magnetisation measurements of the $\text{Gd}_{0.4}\text{Tb}_{0.6}(\text{HCO}_2)_3$ framework.

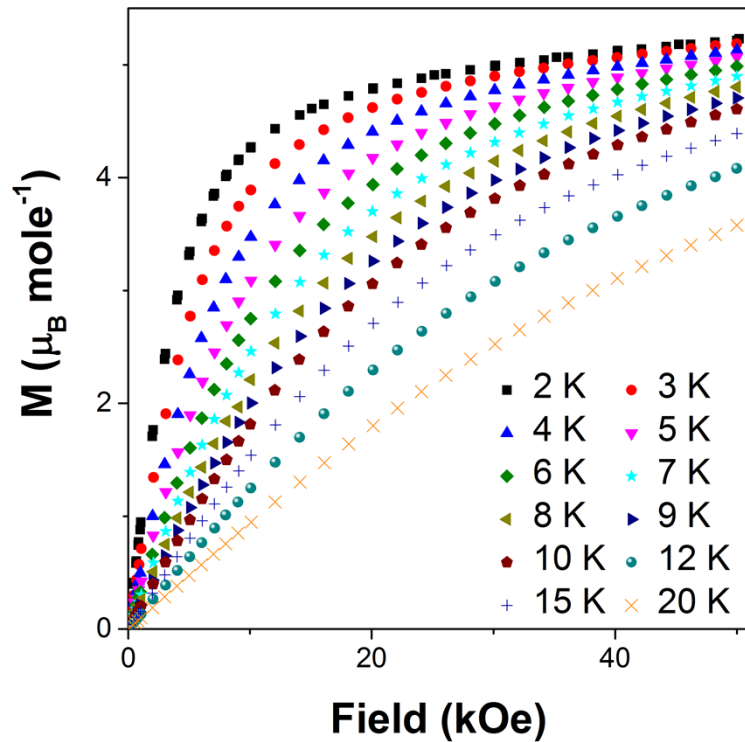


Fig. S22: Isothermal magnetisation measurements of the $\text{Gd}_{0.2}\text{Tb}_{0.8}(\text{HCO}_2)_3$ framework.

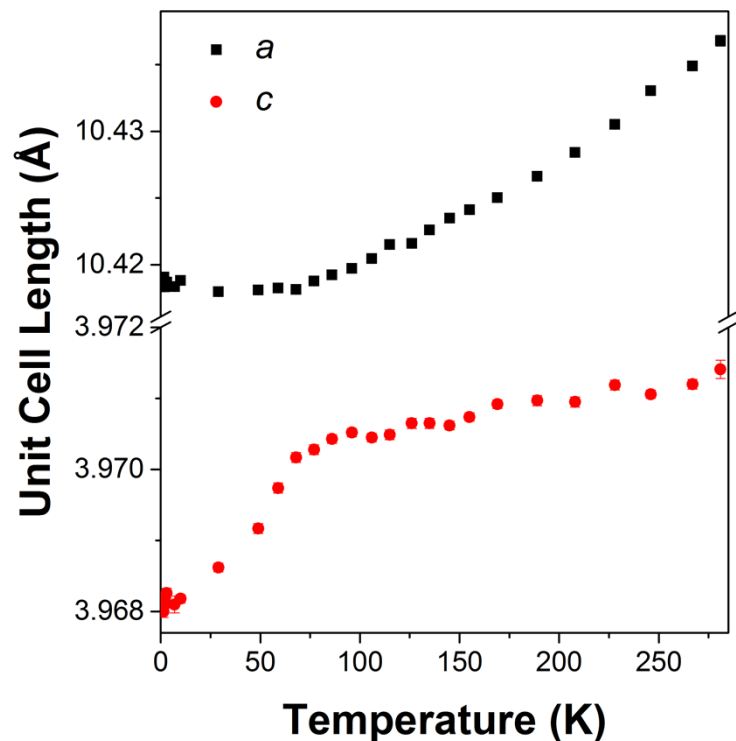


Fig. S24: Unit cell lengths of $\text{Tb}(\text{DCO}_2)_3$ determined from Rietveld fits to neutron diffraction data.

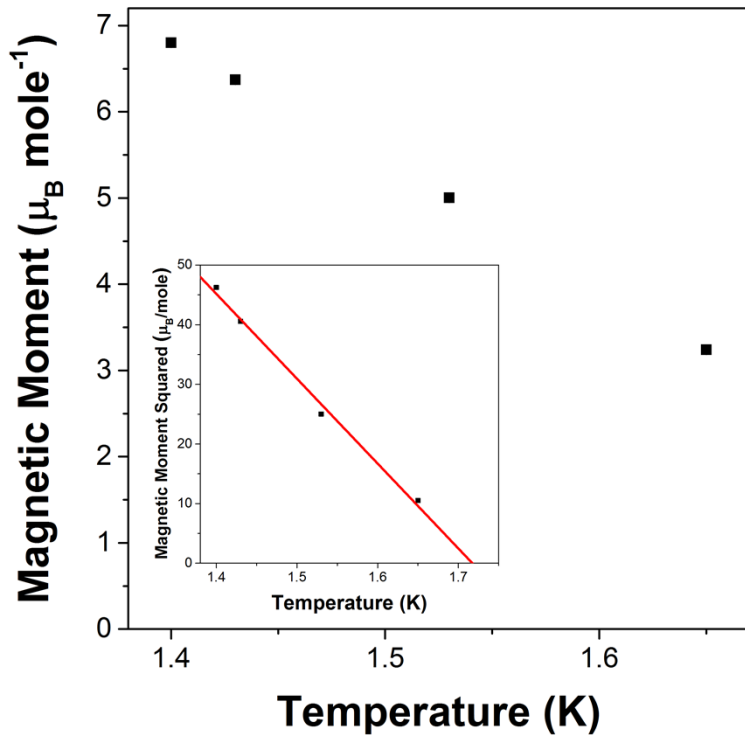


Fig. S25: The main figure represents the evolution of the refined magnetic moment of $\text{Tb}(\text{DCO}_2)_3$ determined from Rietveld fits to neutron diffraction data. The insert presents a linear fit to the square of the magnetic moment, which is proportional to the Landau order parameter, Q .

Table S1: Crystallographic details of $\text{Tb}(\text{DCO}_2)_3$ determined from neutron diffraction data collected at 300 K. Final total refinement statistics R_p and R_{wp} were 2.35 % and 2.57 %.

Space Group	a (Å)	b (Å)	c (Å)	Volume (Å ³)	
$R3m$	10.45307(2)	10.45307(2)	3.97498(7)	376.143(18)	
Site	x	y	z	U_{iso} (Å ²)	Fractional Occupancy
Tb	1/3	2/3	0	-0.0005(3)	1
C	0.51300(6)	0.48700(6)	0.2164(5)	0.0064(3)	1
O1	0.46583(5)	0.53417(5)	-0.0094(4)	0.0052(3)	1
O2	0.58310(5)	0.41690(5)	0.1648(5)	0.0044(2)	1
D	0.49437(7)	0.50563(7)	0.4788(5)	0.0356(5)	1

Table S2: Crystallographic details of $\text{Tb}(\text{DCO}_2)_3$ determined from neutron diffraction data collected at 3 K. Final total refinement statistics R_p and R_{wp} were 1.67 % and 2.30 %.

Space Group	a (Å)	b (Å)	c (Å)	Volume (Å ³)	
$R3m$	10.41863(3)	10.41863(3)	3.96819(4)	373.030(4)	
Site	x	y	z	U_{iso} (Å ²)	Fractional Occupancy
Tb	1/3	2/3	0	-0.0026(3)	1
C	0.51305(7)	0.48695(7)	0.2185(5)	0.00105(3)	1
O1	0.46548(6)	0.53452(6)	-0.0129(5)	0.0004(3)	1
O2	0.58347(6)	0.41653(6)	0.1665(6)	0.0001(2)	1
D	0.49466(7)	0.50534(7)	0.4855(5)	0.0109(4)	1

Table S3: Selected bond distances for each atom in $\text{Tb}(\text{DCO}_2)_3$ refined from neutron diffraction data obtained at 3 and 300 K.

Bond	Distance (Å)	
	3 K	300 K
Tb-O1	$3 \times 2.3859(10)$	$3 \times 2.3998(10)$
Tb-O2	$3 \times 2.4873(19)$	$3 \times 2.4917(16)$
Tb-O2	$3 \times 2.4881(20)$	$3 \times 2.5034(18)$
C-O1	1.2571(16)	1.2391(15)
C-O2	1.2874(12)	1.2856(11)
C-D	1.1103(14)	1.0960(14)

Table S4: Selected bond angles for each atom in $\text{Tb}(\text{DCO}_2)_3$ refined from neutron diffraction data obtained at 3 and 300 K.

Bond Angle	Angle ($^\circ$)	
	3 K	300 K
O1-Tb-O1	$3 \times 119.942(4)$	$3 \times 119.963(2)$
O1-Tb-O2	$6 \times 71.40(4)$	$6 \times 71.65(3)$
O1-Tb-O2	$6 \times 73.46(3)$	$6 \times 73.06(3)$
O1-Tb-O2	$3 \times 125.88(7)$	$3 \times 126.27(6)$
O1-Tb-O2	$3 \times 128.36(8)$	$3 \times 128.27(7)$
O2-Tb-O2	$3 \times 63.11(5)$	$3 \times 63.11(5)$
O2-Tb-O2	$3 \times 63.00(6)$	$3 \times 63.44(6)$
O2-Tb-O2	$3 \times 105.79(4)$	$3 \times 105.46(4)$
O2-Tb-O2	$6 \times 144.893(18)$	$6 \times 144.753(15)$
Tb-O1-C	131.83(10)	132.67(9)
Tb-O2-Tb	105.79(4)	105.46(4)
Tb-O2-C	117.88(11)	117.99(10)
Tb-O2-C	136.33(12)	136.56(10)
O1-C-D	119.55(11)	118.51(10)
O2-C-D	116.61(13)	117.11(12)
O1-C-O2	123.84(13)	124.38(12)